Non-Innocent π Linkers Affect Cooperativity in Hydrogen-Bonded Macrocycles

David Almacellas,[a] Stephanie C. C. van der Lubbe,[b] Alice A. Grosch,[b] Iris Tsagri,[b] Pascal Vermeeren,*[b] Jordi Poater,*[a, c] and Célia Fonseca Guerra*[b]

Rigid, linear π-conjugated acetylene linkers connecting a hydrogen-bond acceptor to a hydrogen-bond donor are established building blocks for self-assembled hydrogen-bonded macrocycles. Kohn-Sham molecular orbital and Voronoi deformation density analyses reveal that the acetylene linker plays an unprecedented, non-innocent role in the cooperativity of these hydrogen-bonded macrocycles. The acetylene linker can abstract electron density from the hydrogen-bond acceptor and donor, due to the linkers' low-lying π-LUMO. As a result, the hydrogen-bond acceptor becomes less negatively charged, which both hampers the cooperativity, as well as the hydrogen bond strength, in the hydrogen-bonded macrocycles. This effect becomes more pronounced when the size of the acetylene linker increases. The findings presented in this work can act as design principles for the development of novel supramolecular macrocycles based on hydrogen bonds.

Introduction

Supramolecular chemistry utilizes molecular recognition and self-assembly processes for non-covalent synthesis.[1] The spontaneous generation of a well-defined structure from a set of molecular building blocks bound by non-covalent interactions allows for the construction of novel materials.[2] Well-known is the application of motifs with strong reversible hydrogen bonds.[3] Also in biological systems, which have inspired synthetic supramolecular chemists, hydrogen bonding is utilized to provide the needed reversibility in association. Well-known is the DNA double helix which is held together by hydrogen bonds between the Watson-Crick base pairs adenine and thymine; and guanine and cytosine.[4,5] Later, it has been found that DNA can also fold into other hydrogen-bonded structures, such as guanine quadruplexes, which consist of layers of four guanines held together by Hoogsteen-type hydrogen bonds.[6]

[a] D. Almacellas, Dr. J. Poater
     Departament de Química Inorgànica i Orgànica & IQTCUB
     Universitat de Barcelona
     Martí i Franquès 1–11, 08028 Barcelona (Spain)
     E-mail: jordi.poater@ub.edu

[b] Dr. S. C. C. van der Lubbe, A. A. Grosch, I. Tsagri, Dr. P. Vermeeren,
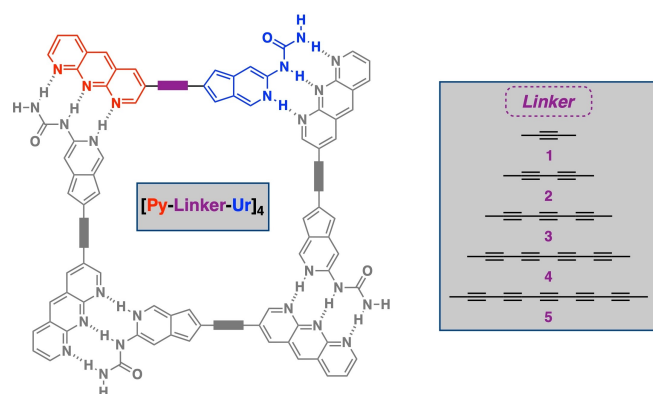   Prof. Dr. C. Fonseca Guerra
     Department of Chemistry and Pharmaceutical Sciences, AIMMS
     Vrije Universiteit Amsterdam
     De Boelelaan 1108, 1081 HZ Amsterdam (The Netherlands)
     E-mail: p.vermeeren@vu.nl
             c.fonsecaguerra@vu.nl

[c] Dr. J. Poater
     ICREA
     Passeig Lluís Companys 23, 08010 Barcelona (Spain)

In our previous work,[7] we showed that hydrogen bonds in these guanine quartets experience a large synergetic effect due to the covalent component, i.e., attractive orbital interactions, in these bonds. The Hoogsteen-type base pair consists of two hydrogen-bond acceptors on one guanine moiety binding with two hydrogen-bond donors on the opposing guanine moiety. Consequently, charge flows within the hydrogen bonds due to the donor–acceptor interactions between the donating σ lone-pair-like orbitals on the oxygen and nitrogen atoms and the accepting σ* orbital on the N–H groups. Note that this mechanism demonstrates the important covalent character of hydrogen bonds.[5,8] This yields a charge separation within the dimer, making the dimer better for subsequent hydrogen bonding than the original monomer. Recently, González-Rodríguez and coworkers[9] obtained hydrogen-bonded assembled quartets by the synthesis of a ditopic monomer which is based on guanosine and cytidine nucleosides at the termini, linked by a linear and rigid π-conjugated p-diethynylbenzene linker. These quartets are prone to self-assemble via a stacking mechanism, thereby forming tubular nanostructures.[9e]

In this work, we propose supramolecular building blocks by taking inspiration from nature which utilizes cooperativity in the guanine quartets and applying to the concept of macrocycles (Scheme 1). We have designed a series of monomers (**Py-Linker-Ur**) constructed from a hydrogen-bond acceptor side, consisting of pyrido[2,3-b][1,8]naphthyridine (**Py**; red), and hydrogen-bond donor side, consisting of 1-(2H-cyclopenta[c]pyridin-3-yl)urea (**Ur**; blue), which are connected by a rigid, linear π-conjugated acetylene linker, comprising of zero to five acetylene units (**Linker**; purple). Four identical monomers can form hydrogen-bonded quartets [**Py-Linker-Ur**]₄, which have their hydrogen bonds pointing all in the same direction. From previous work,[7,10] we know that in such a case, the hydrogen bonding can be strengthened by charge separation in the σ-electronic system through the covalent component in the hydrogen bond and hence demonstrate cooperativity. We want to investigate if these cooperative

Scheme 1. Schematic representation of quartet consisting of monomers with a hydrogen-bond acceptor side, pyrido[2,3-b][1,8]naphthyridine (**Py**; red), and hydrogen-bond donor side, 1-(2H-cyclopenta[c]pyridin-3-yl)urea (**Ur**; blue) with a linear π-conjugated linker of acetylene chain, consisting of zero to five acetylene units (**Linker**; purple).

Figure 1. Geometries of [**Py-Linker-Ur**]$_4$ quartets with different acetylene linkers, including hydrogen bond lengths (in Å) and hydrogen bonding energies, i.e., complexation energy, (in brackets and in kcal mol^{-1}). Computed at ZORA-BLYP-D3(BJ)/TZ2P

effects can hold over a long distance via the π-conjugated linkers and understand the mechanism behind the synergy in the σ- and π- electronic systems. This quantum chemical study using ZORA-BLYP-D3(BJ)/TZ2P[11] is based on a quantitative Kohn-Sham molecular orbital theory together with an energy decomposition analysis (EDA),[12,13] complemented by a Voronoi deformation density (VDD) analysis[14] of the charge distribution to monitor the electronic rearrangements and flow in the formed hydrogen bonds. The goal is to propose design principles for new supramolecular macrocycles.

Results and Discussion

Structure and bond strength in hydrogen-bonded quartets

The optimized structures of our newly designed [**Py-Linker-Ur**]$_4$ quartets based on the diptopic **Py-Linker-Ur** monomers are represented in Figure 1 (see Supporting Information for computational details). The strongest hydrogen bonds, i.e., complexation energy, are obtained for the quartet consisting of the parent monomer without linker **PyUr** and amounts -96.4 kcal mol^{-1}. The hydrogen bonds in the quartet become less stabilizing when the acetylene linker is introduced and continues to decrease when the size of the linker increases, as reflected by the reduction in hydrogen bond strength to -92.5 kcal mol^{-1} for **Py-1-Ur** and to -84.3 kcal mol^{-1} for **Py-5-Ur**. Increasing the linker also affects the hydrogen bond lengths within the quartets. Where the outer and center hydrogen bonds, denoted HB1 and HB2 in Figure 1, respectively, become consistently longer, the inner hydrogen bond HB3 gets shorter going from **PyUr** to **Py-5-Ur**.

By applying the activation strain model (ASM),[15] we pinpoint the interaction energy to be the leading term in determining the trend in hydrogen bond strength in the [**Py-Linker-Ur**]$_4$ quartets upon increasing the size of the acetylene linker (Table 1). In line with the hydrogen bond strength, the interaction energy between the monomers constituting the
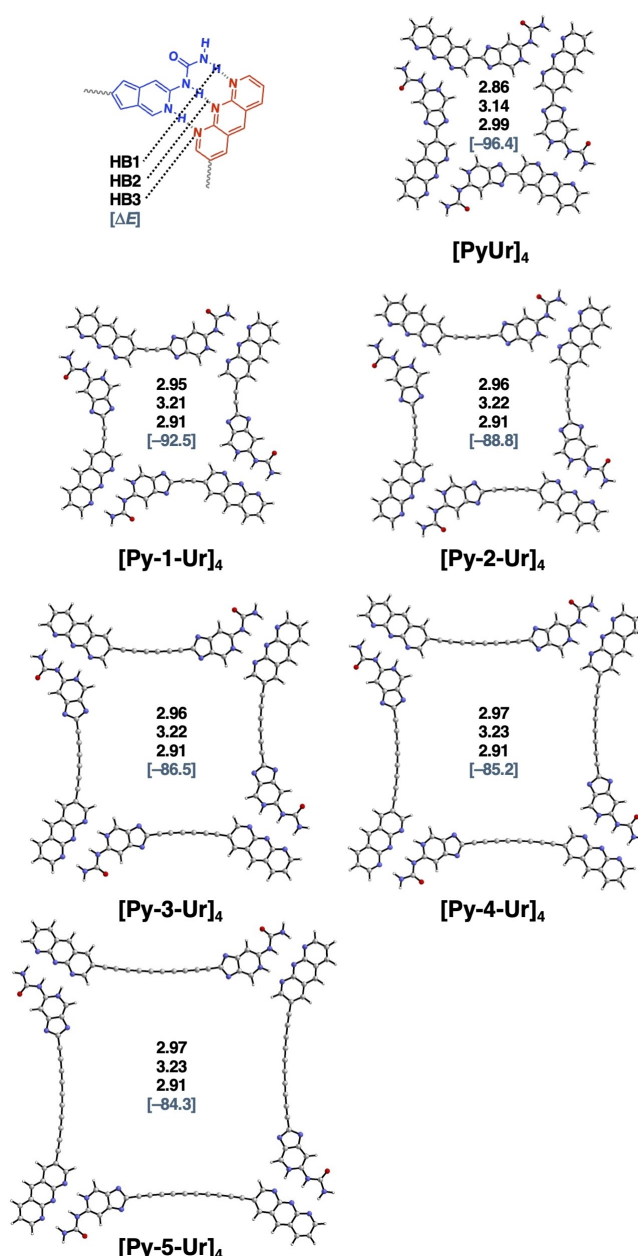
quartets becomes less stabilizing when the size of the linker increases, going from -155.1 kcal mol^{-1} for **PyUr** to -132.0 kcal mol^{-1} for **Py-5-Ur**. The strain energy, on the other hand, shows an opposite trend, since it is the largest and hence most destabilizing for the **PyUr** and nearly consistent for all systems that include an acetylene linker. Nevertheless, for all monomers, most of the strain-induced deformation originates from the dihedral rotation of the **Ur** moiety, which is needed in order to facilitate the formation of the triple-hydrogen bond between the interacting monomers (Figure S1).

To identify the cooperative effect in the hydrogen bonds that constitute the [**Py-Linker-Ur**]$_4$ quartets, we have calculated

Table 1. Bonding and interaction energies (in kcal mol^{-1}) of the [Py-Linker-Ur]$_4$ quartets with different acetylene linkers.[a,b]

System	ΔE	ΔE_{strain}	ΔE_{int}	ΔE_{sum}	ΔE_{syn}
PyUr	−96.4	58.8	−155.1	−138.8	−16.3
Py-1-Ur	−92.5	45.2	−137.6	−126.2	−11.4
Py-2-Ur	−88.8	48.1	−136.8	−127.0	−9.8
Py-3-Ur	−86.5	48.0	−134.5	−125.8	−8.7
Py-4-Ur	−85.2	47.9	−133.1	−125.6	−7.5
Py-5-Ur	−84.3	47.8	−132.0	−124.8	−7.2

[a] Computed at ZORA-BLYP-D3(BJ)/TZ2P. [b] Total complexation energy, *i.e.*, hydrogen bond energy, is computed as: $\Delta E = \Delta E_{strain} + \Delta E_{int}$; and synergy is computed as: $\Delta E_{syn} = \Delta E_{int} - \Delta E_{sum}$. See Computational Details in Supporting Information.

the synergy for all systems by comparing the interaction energy of the quartets with the sum of the pairwise interactions (Table 1). We find that all [Py-Linker-Ur]$_4$ quartets contain a stabilizing cooperative effect as illustrated by the negative ΔE_{syn}. In other words, the hydrogen bonds between the Py-Linker-Ur monomers in the quartet are effectively more stabilizing than the hydrogen bonds in the dimer. The cooperative effect persists under experimental conditions as it still exists in the organic solvent (chloroform) utilized in experiments[9] (Table S9) and, as shown in previous work,[7a,9d,e] remains almost unaffected in layers of stacked systems. The cooperative effect in the quartets, however, becomes consistently less pronounced when the size of the acetylene linker increases, since the synergy reduces from −16.3 kcal mol^{-1} for PyUr to −7.2 kcal mol^{-1} for Py-5-Ur. This demonstrates that increasing the size of the acetylene linker has a predominant effect on the cooperativity. The reason behind this phenomenon will be discussed later.

Nature of bonding in dimers

To fully understand the bonding mechanism underlying the cooperative self-assembly of the hydrogen bonds in the studied [Py-Linker-Ur]$_4$ quartets, we first analyze the formation of the [Py-Linker-Ur]$_2$ dimers, where the geometries are taken from their respective quartets. By utilizing the energy decomposition

analysis (EDA), we establish that the hydrogen bonds are significantly covalent in nature, as the orbital interactions are, in line with our previous work,[5] more than half of the magnitude of the electrostatic interactions (Table 2). Notably, the orbital interaction stems mainly from the charge transfer within the σ-orbital system, nevertheless, the polarization in the π-orbital interaction is, as a result of the extended π-systems of the Py-Linker-Ur monomers, not negligible.

The trend in interaction energy along the series is due to a combination of both a reduced stabilizing electrostatic and orbital interactions that make the hydrogen bond in the dimer weaker when the size of the acetylene linker increases. Table 2 shows that the hydrogen-bond interaction energy in the dimer weakens upon increasing the linker size from −34.0 kcal mol^{-1} for PyUr to −31.1 kcal mol^{-1} for Py-5-Ur. This trend in interaction energy is originating from electrostatic interactions with a smaller contribution of the orbital interactions. The latter energy term especially plays a role going from PyUr to Py-1-Ur. The dispersion interaction and Pauli repulsion, on the other hand, remain constant or show even an opposite trend and hence are not responsible for the observed trend in interaction energy.

A detailed Voronoi deformation density (VDD) analysis[14] reveals that it is, in fact, the non-innocent role of the acetylene linker that leads to a weakening of the stabilizing electrostatic and orbital interactions in forming the dimer when increasing the size of the acetylene linker. The acetylene linker is able to better accept electronic density when it increases, due to its consistently more stabilizing π^*_{LUMO} orbital.[16] As a result, the hydrogen-bond acceptor Py becomes positively charged, going from −30 milli-electrons for PyUr to +59 milli-electrons for Py-5-Ur (Figure 2). This effectively hampers the electrostatic interaction with the already positively charged hydrogen-bond donor Ur, which becomes, due to the acetylene linker, even more positively charged.

Furthermore, the positive charge on the Py moiety of Py-Linker-Ur induced by the acetylene linker also has a destabilizing effect on the orbital interactions (See Figure 3 for bonding mechanism). This is most apparent when going from PyUr to Py-1-Ur, where the orbital interaction on Py goes from −20.3 to −19.0 kcal mol^{-1}. The accumulation of positive charge on Py results in a stabilization of the $\sigma_{HOMO,Py}$ hydrogen-bond accepting orbitals on the Py moiety from −5.3 eV, −5.5 eV, and

Table 2. Energy decomposition analysis of the hydrogen bond in the [Py-Linker-Ur]$_2$ dimers with different acetylene linkers (in kcal mol^{-1}).[a,b,c]

System	ΔE_{int}	ΔV_{elstat}	ΔE_{Pauli}	ΔE_{σ}	ΔE_{π}	ΔE_{oi}	ΔE_{disp}
PyUr	−34.0	−42.3	40.6	−20.3	−3.9	−24.2	−8.1
Py-1-Ur	−32.1	−38.7	37.6	−19.0	−3.7	−22.7	−8.2
Py-2-Ur	−31.6	−37.7	36.7	−18.7	−3.8	−22.4	−8.1
Py-3-Ur	−31.3	−37.0	36.2	−18.5	−3.8	−22.4	−8.1
Py-4-Ur	−31.2	−36.7	36.0	−18.5	−3.9	−22.4	−8.1
Py-5-Ur	−31.1	−36.4	35.7	−18.4	−4.0	−22.4	−8.1

[a] Computed at ZORA-BLYP-D3(BJ)/TZ2P. [b] Geometries of dimers taken from the optimized quartets. [c] Interaction energy is decomposed as: $\Delta E_{int} = \Delta V_{elstat} + \Delta E_{Pauli} + \Delta E_{oi} + \Delta E_{disp}$. See Computational Details in Supporting Information.
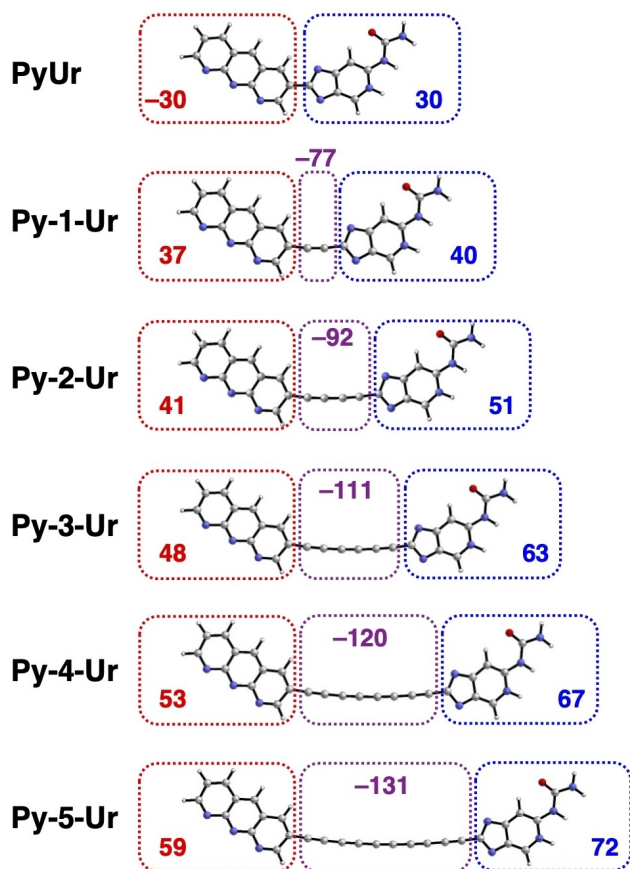
Figure 2. Voronoi deformation density (VDD) charges Q (in milli-electrons) for the **Py-Linker-Ur** monomers in the geometry of the optimized quartet, where the total VDD charge on the hydrogen-bond acceptor (**Py**; red), acetylene linker (**Linker**; purple), and hydrogen-bond donor (**Ur**; blue) are given. Computed at ZORA-BLYP-D3(BJ)/TZ2P.

−5.8 eV for **PyUr** to −5.5 eV, −5.7 eV, and −6.2 eV for **Py-1-Ur**. This, consequently, gives rise to larger σ-HOMO–σ-LUMO orbital energy gaps between the monomers upon forming the dimer and hence weakens the orbital interactions. Thus, introducing an acetylene linker, and by elongation thereof, the hydrogen bond of the [**Py-Linker-Ur**]$_2$ dimers gets weaker, due to the electron acceptance capability of the acetylene linker, thereby weakening the stabilizing electrostatic and orbital interactions between the interacting monomers.

Cooperativity in the hydrogen-bonded quartets

Next, we investigate the origin of cooperativity in the [**Py-Linker-Ur**]$_4$ quartets by stepwise adding a monomer to the system, i.e., M_2 = monomer + monomer, M_3 = dimer + monomer, M_4 = trimer + monomer. Here, we are analyzing the quartets constructed from the monomers **PyUr**, **Py-1-Ur**, and **Py-5-Ur** (Table 3). All other quartets have the same characteristics and can be found in Table S2. As mentioned above, all systems contain a stabilizing cooperativity as illustrated by the negative ΔE_{syn}. This cooperative effect in the quartets, however, becomes consistently smaller when the size of the acetylene linker increases. By performing the energy decomposition analysis (EDA),[13] we find that the main contributors to the synergy, as well as the trend therein, are the electrostatic and orbital interactions, as these energy terms become consistently more stabilizing upon stepwise formation of the system but weaker when the length of the acetylene linker increases. Interestingly, although the σ-orbital interaction is the strongest in these hydrogen bonds, the π-orbital interaction has a larger synergy. Nevertheless, the reduction of this stabilizing effect when the size of the acetylene linker increases is larger for the former than the latter orbital interaction.
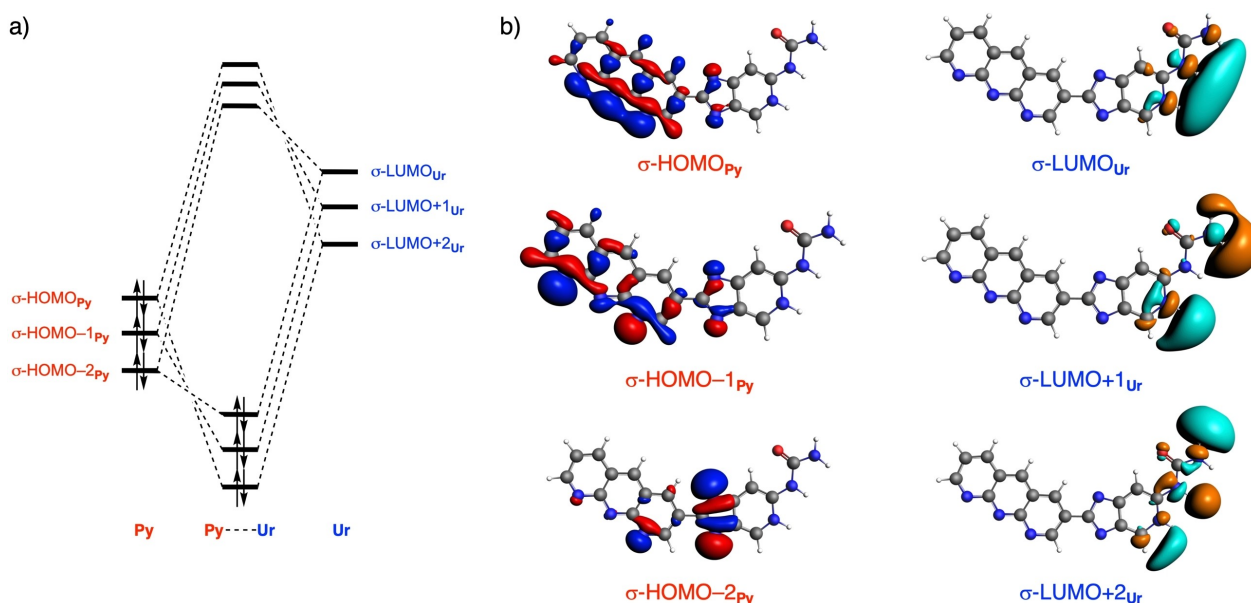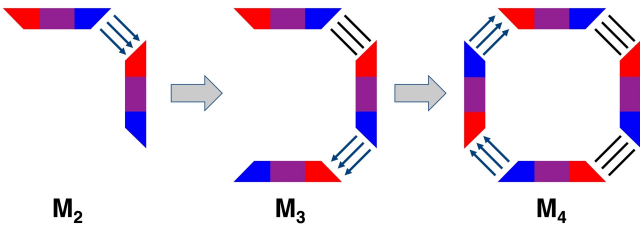

Figure 3. a) Schematic molecular orbital diagram of the hydrogen bond formation between the **Py** and **Ur** moiety of two interacting monomers; b) key σ-orbitals (isovalue = 0.03 Bohr$^{-3/2}$) located on the monomer of **PyUr** that interact upon forming the dimer.

Table 3. Energy decomposition analysis and synergy (in kcal mol^{-1}) of the stepwise formation of the **[Py-Linker-Ur]$_4$** quartets with different acetylene linkers.[a,b,c]

System		$\triangle E_{int}$	$\triangle V_{elstat}$	$\triangle E_{Pauli}$	$\triangle E_{\sigma}$	$\triangle E_{\pi}$	$\triangle E_{oi}$	$\triangle E_{disp}$
PyUr	**M$_2$**	−34.0	−42.3	40.6	−20.3	−3.9	−24.2	−8.1
	M$_3$	−39.1	−45.5	40.4	−21.2	−4.8	−26.0	−8.1
	M$_4$	−82.0	−90.6	81.3	−44.0	−12.5	−56.6	−16.2
	$\triangle E_{syn}$	−16.3	−6.3	−0.1	−4.2	−5.6	−9.8	0.0
Py-1-Ur	**M$_2$**	−32.1	−38.7	37.6	−19.0	−3.7	−22.7	−8.2
	M$_3$	−35.4	−40.6	37.4	−19.6	−4.5	−24.1	−8.2
	M$_4$	−73.8	−81.2	75.2	−40.1	−11.4	−51.5	−16.4
	$\triangle E_{syn}$	−11.4	−4.6	−0.1	−2.6	−4.6	−7.2	−0.0
Py-5-Ur	**M$_2$**	−31.1	−36.4	35.7	−18.4	−4.0	−22.4	−8.1
	M$_3$	−32.9	−37.2	35.7	−18.8	−4.5	−23.3	−8.1
	M$_4$	−68.1	−74.7	71.5	−38.0	−10.6	−48.6	−16.2
	$\triangle E_{syn}$	−7.2	−1.6	−0.1	−1.6	−3.2	−4.8	0.0

[a] Computed at ZORA-BLYP-D3(BJ)/TZ2P. [b] **M$_2$** = monomer + monomer, **M$_3$** = dimer + monomer, **M$_4$** = trimer + monomer. [c] See Table S2 for the analyses of all **[Py-Linker-Ur]$_4$** quartets.

Both the synergy in the electrostatic and orbital interactions originate from charge transfer between the occupied and unoccupied orbitals of the interacting fragments, leading to an increased charge separation in the system. This charge separation becomes smaller for the systems with a larger acetylene linker. The Voronoi deformation density (VDD) charge analysis[14] quantifies the charge transfer between the monomers that constitute the quartets. Upon stepwise formation of the **[Py-Linker-Ur]$_4$** quartets, the σ-donor–acceptor interactions between the hydrogen-bond donor and hydrogen-bond acceptor leads to a charge transfer between the interacting fragments (Figure 4). Resultingly, charge flows from one terminal monomer to the other terminal monomer leading to charge separation in the system, which systematically increases upon stepwise formation of the quartet. This charge transfer between the fragments, however, becomes less pronounced when the acetylene linker is introduced, due to the prior discussed electron acceptance capability of the acetylene linker, which makes the hydrogen-bond acceptor positively charged. Thus, for these systems, the charge transfer is initially already weaker than for **PyUr**, and constructing the quartet will only make the charge separation less pronounced.

As a result of the charge separation in the system, the hydrogen-bond acceptor becomes more negatively charged, whereas the hydrogen-bond donor becomes more positively charged (Figure 5). This effect is most prominent when the dimer **M$_2$** is formed and only small upon forming the trimer **M$_3$**. For example, the hydrogen-bond acceptor of **PyUr** becomes increasingly more negatively charged from −30 to −81 to −86 milli-electrons from **M** to **M$_2$** to **M$_3$**, whereas the hydrogen-bond donor becomes more positively charged from 30 to 86 to 92 milli-electrons along the same series. This effect, again, becomes less prominent when the size of the acetylene linker increases.

The charge separation upon stepwise formation of the quartet, because of the charge transfer, also causes the synergy in the σ-orbital interactions. Kohn-Sham molecular orbital (KS-MO) analysis[12] shows that the accumulation of charge on the terminal hydrogen-bond acceptor (**Py**) and donor (**Ur**) affects the orbital energies of the orbitals involved in the hydrogen bonds located on these termini. The increasing negative charge on the terminal hydrogen-bond acceptor **Py** destabilizes, *i.e.*, an increase in energy, the σ-HOMOs (Table 4). For instance, the σ-HOMOs of **PyUr** go from −5.3, −5.5, and −5.8 eV in **M** to −4.8, −4.9, and −5.2 eV in **M$_3$**. The σ-LUMOs, on the other hand, become stabilized, due to the increased positive charge on the terminal hydrogen-bond donor **Ur**. For example, the σ-LUMOs of **PyUr** go from −2.1, −1.2, and −0.2 eV in **M** to −2.4, −1.5, and −0.5 eV in **M$_3$**. As a result, the HOMO–LUMO energy gap between the interacting fragments becomes smaller, leading to enhanced σ-orbital interactions.

In addition, the charge separation within the system also promotes the π-orbital interaction. The increased negative charge on hydrogen-bond acceptor and positive charge on the hydrogen-bond donor not only destabilizes and stabilizes the σ-HOMO and σ-LUMO, respectively, but also the π-HOMO and
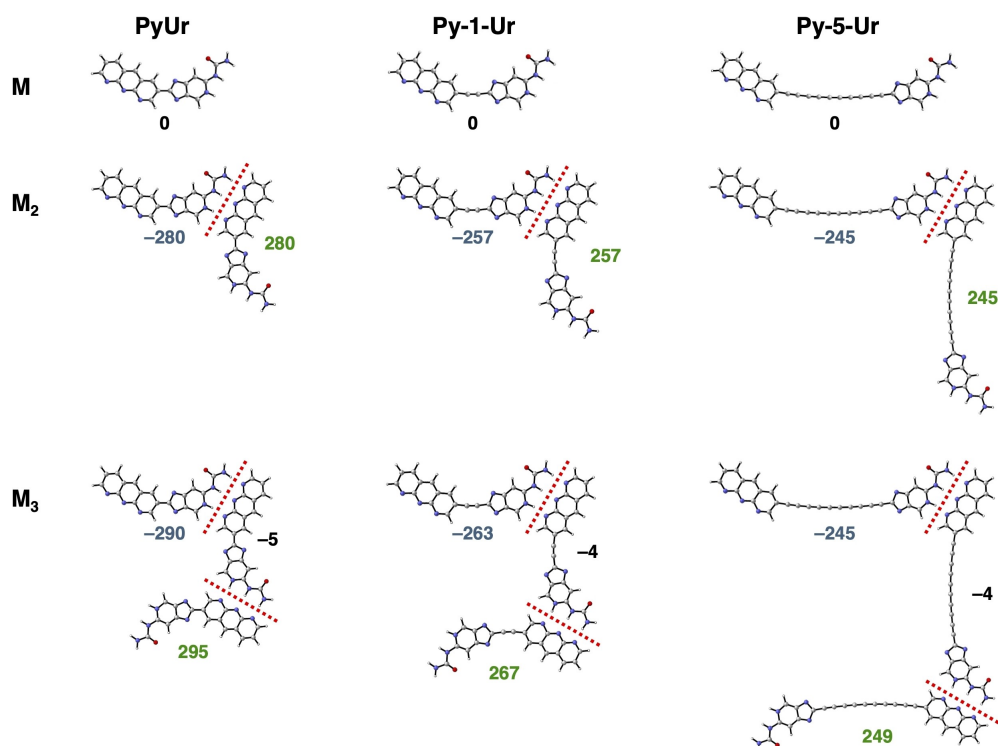
Figure 4. VDD charges Q (in milli-electrons) of the monomers upon stepwise formation of the [PyUr]$_4$, [Py-1-Ur]$_4$, and [Py-5-Ur]$_4$ quartets, computed at ZORA-BLYP-D3(BJ)/TZ2P.
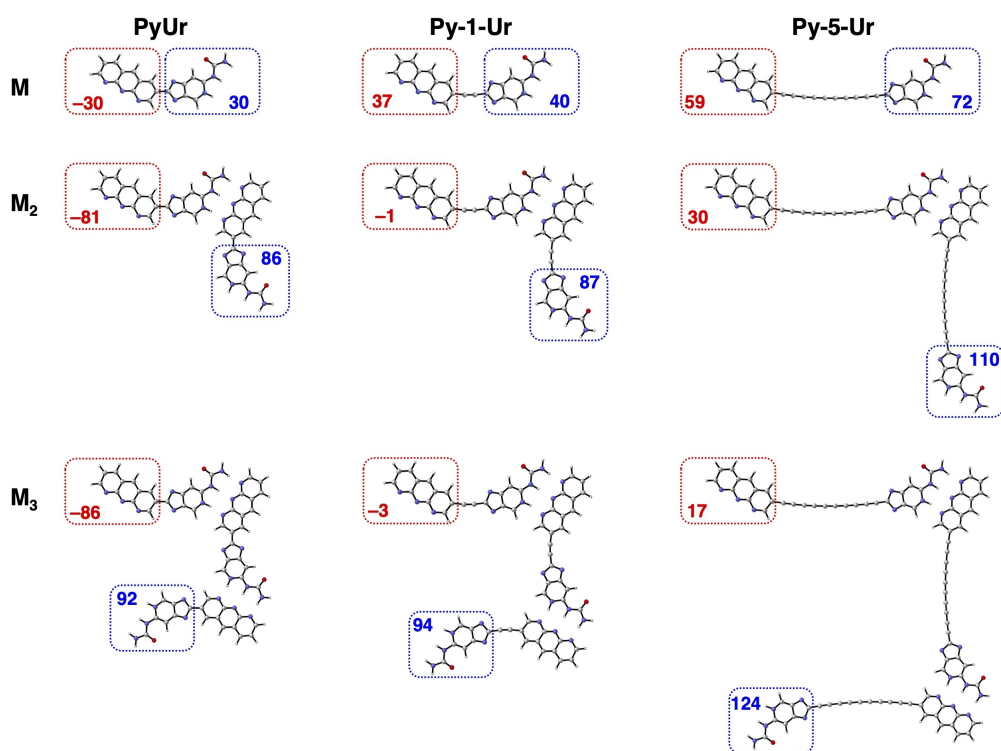

Figure 5. VDD charges Q (in milli-electrons) of the terminal hydrogen-bond acceptor (**Py**; red) and hydrogen-bond donor (**Ur**; blue) for fragments upon stepwise formation of the [PyUr]$_4$, [Py-1-Ur]$_4$, and [Py-5-Ur]$_4$ quartets, computed at ZORA-BLYP-D3(BJ)/TZ2P.

π-LUMO of the monomers. Thus, building the quartet significantly reduces the π-HOMO–LUMO gap, thereby enhancing the

π-polarization (Tables S3 and S4). The effect on the orbital energies, however, becomes less pronounced when the

Table 4. [VP(1)]
Orbital energies of key orbitals (in eV) participating in the hydrogen bond for fragments of the **[PyUr]**$_4$, **[Py-1-Ur]**$_4$, and **[Py-5-Ur]**$_4$ quartets, where the σ-HOMOs are located on the hydrogen-bond acceptor (**Py**) and the σ-LUMOs on the hydrogen-bond donor (**Ur**).[a]

System		$\sigma_{HOMO,Py}$	$\sigma_{HOMO-1,Py}$	$\sigma_{HOMO-2,Py}$	$\sigma_{LUMO, Ur}$	$\sigma_{LUMO-1, Ur}$	$\sigma_{LUMO-2, Ur}$
PyUr	M	−5.3	−5.5	−5.8	−2.1	−1.2	−0.2
	M$_2$	−4.8	−4.9	−5.1	−2.4	−1.5	−0.5
	M$_3$	−4.8	−4.9	−5.2	−2.4	−1.5	−0.5
Py-1-Ur	M	−5.5	−5.7	−6.2	−2.1	−1.2	−0.2
	M$_2$	−5.2	−5.4	−5.8	−2.3	−1.4	−0.4
	M$_3$	−5.2	−5.4	−5.9	−2.3	−1.4	−0.4
Py-5-Ur	M	−5.8	−6.0	−6.5	−2.1	−1.2	−0.2
	M$_2$	−5.6	−5.7	−6.2	−2.3	−1.4	−0.4
	M$_3$	−5.6	−5.7	−6.2	−2.3	−1.4	−0.4

[a] Computed at ZORA-BLYP-D3(BJ)/TZ2P.

acetylene linker increases, in line with the above-mentioned reduced charge transfer. This, ultimately, leads to less synergy in both the σ- and π-orbital interaction when the linker becomes longer.

Expanding towards phenyl linkers

In the final section of this manuscript, we examine the effect of using a phenyl linker (**Py-Ph-Ur**) and an acetylene-phenyl-acetylene linker (**Py-1-Ph-1-Ur**) between the hydrogen-bond acceptor and donor, which are frequently used by González-Rodríguez et al (Figure 6).[9]
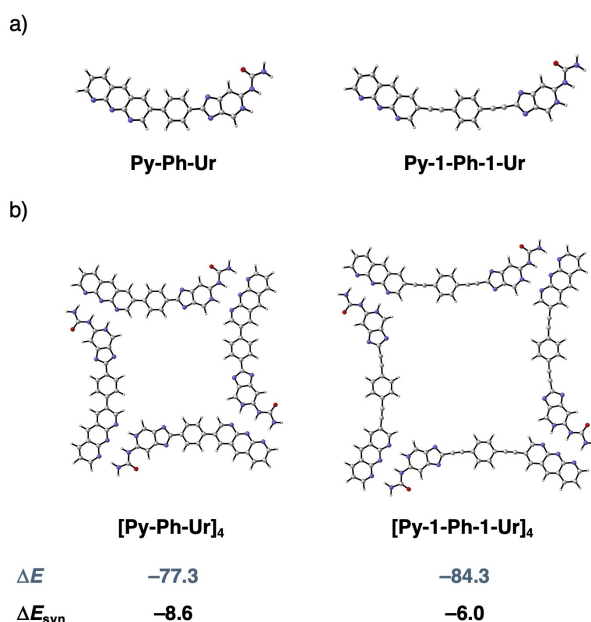
a)

Py-Ph-Ur   **Py-1-Ph-1-Ur**

b)

[Py-Ph-Ur]$_4$ **[Py-1-Ph-1-Ur]**$_4$

ΔE	−77.3	−84.3
ΔE_{syn}	−8.6	−6.0

Figure 6. Geometries of a) monomers with phenyl linker (**Py-Ph-Ur**) and acetylene-phenyl-acetylene linker (**Py-1-Ph-1-Ur**); and b) their respective quartets with hydrogen bonding energy and synergy (in kcal mol^{-1}). Computed at ZORA-BLYP-D3(BJ)/TZ2P.

In analogy with linking the hydrogen-bond donor and acceptor with an acetylene linker, connecting them with a phenyl **Py-Ph-Ur** or acetylene–phenyl–acetylene linker **Py-1-Ph-1-Ur** results in a weakening of the hydrogen bond strength in the quartet from −96.4 kcal mol^{-1} for **PyUr** to −77.3 and −84.3 kcal mol^{-1} for **Py-Ph-Ur** and **Py-1-Ph-1-Ur**, respectively. The quartets constructed from these monomers benefit from a stabilizing cooperativity as illustrated by the negative ΔE_{syn}, which, in turn, originates from the strengthening of the electrostatic interaction and orbital interactions upon building the quartet (Table S5). Nevertheless, the cooperativity of these systems is significantly less pronounced compared to the quartet constructed from the parent monomer without any linker. This is due to the non-innocent role of the phenyl linker, which, in contrast to the acetylene linker, donates electron density towards the termini. As a result, the hydrogen-bond donor **Ur** becomes less positively charged, going from +30 milli-electrons for **PyUr** to +10 milli-electrons for **Py-Ph-Ur** (Figure S2), thereby, hampering both the hydrogen bond strength and cooperativity in these systems. Using an acetylene–phenyl–acetylene linker as in **Py-1-Ph-1-Ur** somewhat counteracts this phenomenon, due to the acetylene moieties, making it act more like the original acetylene linkers discussed above.

Conclusions

In this work, we have demonstrated and explained the origin of cooperativity in a series of hydrogen-bonded macrocycles consisting of a hydrogen-bond acceptor side and a hydrogen-bond donor side, which are connected by a rigid, linear π-conjugated acetylene linker of different lengths. All studied macrocycles show a cooperative effect, but the magnitude thereof becomes less stabilizing upon increasing the size of the acetylene linker. This follows from our dispersion-corrected density functional theory (DFT-D) calculations based on quantitative Kohn-Kohn molecular orbital theory and Voronoi deformation density (VDD) analyses.

Our analyses reveal that the cooperativity in the formation of the macrocyclic quartets stems from charge transfer between the occupied and unoccupied σ-orbitals of the interacting fragments, leading to an increased charge separation in the system. Importantly, the acetylene linker plays a non-innocent role in the formation of the macrocyclic quartets. As the size of the acetylene linker increases, it is able to abstract electron density from the terminal hydrogen-bond acceptor and donor due to a consistently more stable π-LUMO. As a result, the termini become positively charged, which both hampers the hydrogen bond strength, as well as the cooperativity, in the hydrogen-bonded macrocycles with increasing linker size.

Finally, this work demonstrates that our findings are also applicable to the hydrogen-bonded macrocycles containing the experimentally viable linker synthesized by González-Rodríguez *et al*.[9] We, therefore, envision that the herein obtained findings can act as design principles for the development of novel supramolecular macrocycles based on hydrogen bonds.

Experimental Section

All calculations were carried out using the Amsterdam Density Functional (ADF) program (version 2019.301).[17] All stationary points and energies were calculated at the BLYP level of the generalized gradient approximation (GGA): exchange functional developed by Becke (B) and the GGA correlation functional developed by Lee, Yang, and Parr (LYP).[18] The DFT-D3(BJ) method developed by Grimme and coworkers,[19] which contains the damping function proposed by Becke and Johnson,[20] is used to describe non-local dispersion interactions. Scalar relativistic effects are accounted for using the zeroth-order regular approximation (ZORA).[21] This level is referred to as ZORA-BLYP-D3(BJ)/TZ2P and has been proven to accurately describe weak interactions.[7c,10c,22] A large uncontracted optimized TZ2P Slater type orbitals (STOs) basis set containing diffuse functions were used. The TZ2P all-electron basis set,[23] with no frozen-core approximation, is of triple-ζ quality for all atoms and has been augmented with two sets of polarization functions on each atom. The accuracies of the integration grid (Becke grid) and the fit scheme (Zlm fit) were set to VERYGOOD.[24] All calculations above have been performed in vacuo. In addition, the effect of solvation in chloroform has been tested for [PyUr]$_4$ quartet at the same ZORA-BLYP-D3(BJ)/TZ2P level including Conductor like Screening Model (COSMO) of solvation[25] (Tables S9 and S10).

Conflict of Interests

There are no conflicts to declare.

Data Availability Statement

The data that support the findings of this study are available in the supplementary material of this article.

[1] J. Lehn, *Supramolecular Chemistry*; VCH: Weinheim, **1995**.
[2] a) G. R. Desiraju, *Angew. Chem. Int. Ed.* **1995**, *42*, 2311; b) R. Chakrabarty, P. S. Mukherjee, P. J. Stang, *Chem. Rev.* **2011**, *111*, 6810; c) A. del Prado, D. González-Rodríguez, Y.-L. Wu, *ChemistryOpen* **2020**, *9*, 409.
[3] a) F. H. Beijer, R. P. Sijbesma, H. Kooijman, A. L. Spek, E. W. Meijer, *J. Am. Chem. Soc.* **1998**, *120*, 6761; b) S. H. M. Söntjes, R. P. Sijbesma, M. H. P. van Genderen, E. W. Meijer, *J. Am. Chem. Soc.* **2000**, *122*, 7487; c) W. P. J. Appel, M. M. L. Nieuwenhuizen, M. Lutz, B. F. M. de Waal, A. R. A. Palmans, E. W. Meijer, *Chem. Sci.* **2014**, *5*, 3735; d) H. Coubrough, S. C. C van der Lubbe, K. Parashiv, A. Minard, C. Pask, M. Howard, C. Fonseca Guerra, A. J. Wilson, *Chem. Eur. J.* **2019**, *25*, 785.
[4] a) J. M. Berg, J. L. Tymoczko, L. Stryer, *Biochemistry, 5th Edition*, W. H. Freeman and Company, New York, **2002**; b) W. Saenger, *Principles of Nucleic Acid Structure*, Springer, New York, **1984**, p. 122.
[5] a) C. Fonseca Guerra, F. M. Bickelhaupt, J. G. Snijders, E. J. Baerends, *Chem. Eur. J.* **1999**, *5*, 3581; b) C. Fonseca Guerra, F. M. Bickelhaupt, *Angew. Chem. Int. Ed.* **1999**, *38*, 2942; c) C. Fonseca Guerra, F. M. Bickelhaupt, *Angew. Chem. Int. Ed.* **2002**, *41*, 2092; d) C. Nieuwland, F. Zaccaria, C. Fonseca Guerra, *Phys. Chem. Chem. Phys.* **2020**, *22*, 21108; e) C. Nieuwland, T. A. Hamlin, C. Fonseca Guerra, G. Barone, F. M. Bickelhaupt, *ChemistryOpen* **2022**, *11*, e202100231; f) T. A. Hamlin, J. Poater, C. Fonseca Guerra, F. M. Bickelhaupt, *Phys. Chem. Chem. Phys.* **2017**, *19*, 16969.
[6] a) L. Stefan, D. Monchaud, *Nat. Chem. Rev.* **2019**, *3*, 650; b) M. L. Bochman, K. Paeschke, V. A. Zakian, *Nat. Rev. Genet.* **2012**, *13*, 770; c) J. T. Davis, *Angew. Chem., Int. Ed.* **2004**, *43*, 668; d) C. Nieuwland, C. Fonseca Guerra, in *Modern Avenues in Metal-Nucleic Acid Chemistry. Metal Ions in Life Sciences* (Eds. J. Müller, B. Lippert, A. Sigel, H. Sigel, E. Freisinger, R. K. O. Sigel), CRC Press: Boca Raton, **2023**, *25*, pp 343–372; e) Á. Sánchez-González, N. A. G. Bandeira, I. Ortiz de Luzuriaga, F. F. Martins, S. Elleuchi, K. Jarraya, J. Lanuza, X. Lopez, M. J. Calhorda, A. Gil, *Molecules* **2021**, *26*, 4737; f) I. Ortiz de Luzuriaga, Á. Sánchez-González, W. Synoradzki, X. Lopez, A. Gil, *Phys. Chem. Chem. Phys.* **2022**, *24*, 25918.
[7] a) C. Fonseca Guerra, H. Zijlstra, G. Paragi, F. M. Bickelhaupt, *Chem. Eur. J.* **2011**, *17*, 12612; b) G. Paragi, C. Fonseca Guerra, *Chem. Eur. J.* **2017**, *23*, 3042; c) F. Zaccaria, S. C. C. van der Lubbe, C. Nieuwland, T. A. Hamlin, C. Fonseca Guerra, *ChemPhysChem* **2021**, *22*, 2265.
[8] a) H. Umeyama, K. Morokuma, *J. Am. Chem. Soc.* **1977**, *99*, 1316; b) S. Yamabe, K. Morokuma, *J. Am. Chem. Soc.* **1975**, *97*, 4458; c) K. Morokuma, *Acc. Chem. Res.* **1977**, *10*, 294; d) S. C. C. van der Lubbe, C. Fonseca Guerra, *Chem. Asian J.* **2019**, *14*, 2769.
[9] a) C. Montoro-García, N. Bilbao, I. M. Tsagri, F. Zaccaria, M. J. Mayoral, C. Fonseca Guerra, D. González-Rodríguez, *Chem. Eur. J.* **2018**, *24*, 11983; b) C. Montoro-García, M. J. Mayoral, R. Chamorro, D. González-Rodrígues *Angew. Chem. Int. Ed.* **2017**, *56*, 15649; c) D. Serrano-Molina, C. Montoro-García, M. J. Mayoral, A. de Juan, D. González-Rodríguez, *J. Am. Chem. Soc.* **2022**, *144*, 5450; d) M. J. Mayoral, N. Bilbao, D. González-Rodrígues, *ChemistryOpen* **2016**, *5*, 10; e) M. González-Sánchez, M. J. Mayoral, V. Vázquez-González, M. Paloncýová, I. Sancho-Casado, F. Aparicio, A. de Juan, G. Longhit, P. Norman, M. Linares, D. González-Rodrígues, *J. Am. Chem. Soc.* **2023**, *145*, 17805.
[10] a) L. P. Wolters, N. W. G. Smits, C. Fonseca Guerra, *Phys. Chem. Chem. Phys.* **2015**, *17*, 1585; b) J. Dominikowska, F. M. Bickelhaupt, M. Palusiak, C. Fonseca Guerra, *ChemPhysChem* **2016**, *17*, 474; c) P. Vermeeren, L. P. Wolters, G. Paragi, C. Fonseca Guerra, *ChemPlusChem* **2021**, *86*, 812; d) L. de Azevedo Santos, D. Cesario, P. Vermeeren, S. C. C. van der Lubbe, F. Nunzi, C. Fonseca Guerra, *ChemPlusChem* **2022**, *86*, e202100436; e) A. N. Petelski, C. Fonseca Guerra, *ChemistryOpen* **2018**, *8*, 134; f) A. N. Petelski, C. Fonseca Guerra, *Chem. Asian J.* **2022**, *17*, e202201010.
[11] a) A. D. Becke, *Phys. Rev. A* **1988**, *38*, 3098; b) C. Lee, W. Yang, R. G. Parr, *Phys. Rev. B* **1988**, *37*, 785; c) S. Grimme, J. Antony, S. Ehrlich, H. Krieg, *J. Chem. Phys.* **2010**, *132*, 154104; d) S. Grimme, S. Ehrlich, L. Goerigk, *J. Comput. Chem.* **2011**, *32*, 1456; e) E. R. Johnson, A. D. Becke, *J. Chem. Phys.* **2005**, *123*, 024101; f) E. van Lenthe, E. J. Baerends, *J. Comput.*

Chem. **2003**, *24*, 1142; g) E. van Lenthe, E. J. Baerends, J. G. Snijders, *J. Chem. Phys.* **1993**, *99*, 4597; h) E. van Lenthe, E. J. Baerends, J. G. Snijders, *J. Chem. Phys.* **1994**, *101*, 9783; i) E. van Lenthe, A. Ehlers, E. J. Baerends, *J. Chem. Phys.* **1999**, *110*, 8943.

[12] a) T. A. Albright, J. K. Burdett, M.-H. Whangbo, *Orbital Interactions in Chemistry*, John Wiley & Sons, Inc., **2013**; b) R. van Meer, O. V. Gritsenko, E. J. Baerends, *J. Chem. Theory Comput.* **2014**, *10*, 4432.

[13] a) F. M. Bickelhaupt, E. J. Baerends in *Reviews in Computational Chemistry* (Eds.: K. B. Lipkowitz, D. B. Boyd), Wiley, Hoboken, **2000**, pp. 1–86; b) T. A. Hamlin, P. Vermeeren, C. Fonseca Guerra, F. M. Bickelhaupt in *Complementary Bonding Analysis*, (Ed.: S. Grabowsky), De Gruyter, Berlin, **2021**, pp 199–212.

[14] a) C. Fonseca Guerra, J.-W. Handgraaf, E. J. Baerends, F. M. Bickelhaupt, *J. Comput. Chem.* **2004**, *25*, 189; b) C. Nieuwland, P. Vermeeren, F. M. Bickelhaupt, C. Fonseca Guerra *J. Comput. Chem.* **2023**, *44*, e202300379.

[15] a) F. M. Bickelhaupt, K. N. Houk, *Angew. Chem. Int. Ed.* **2017**, *56*, 10070; b) P. Vermeeren, S. C. C. van der Lubbe, C. Fonseca Guerra, F. M. Bickelhaupt, T. A. Hamlin, *Nat. Protoc.* **2020**, *15*, 649; c) P. Vermeeren, T. A. Hamlin, F. M. Bickelhaupt, *Chem. Commun.* **2021**, *57*, 5880.

[16] C. Fonseca Guerra, Z. Szekeres, F. M. Bickelhaupt, *Chem. Eur. J.* **2011**, *17*, 8816.

[17] a) G. te Velde, F. M. Bickelhaupt, E. J. Baerends, C. Fonseca Guerra, S. J. A. van Gisbergen, J. G. Snijders, T. Ziegler, *J. Comput. Chem.* **2001**, *22*, 931; b) C. Fonseca Guerra, J. G. Snijders, G. te Velde, E. J. Baerends, *Theor. Chem. Acc.* **1998**, *99*, 391; c) ADF2019.302, SCM Theoretical Chemistry, Vrije Universiteit, Amsterdam, The Netherlands, www.scm.com.

[18] a) A. D. Becke, *Phys. Rev. A* **1988**, *38*, 3098; b) C. Lee, W. Yang, R. G. Parr, *Phys. Rev. B* **1988**, *37*, 785.

[19] a) S. Grimme, J. Antony, S. Ehrlich, H. Krieg, *J. Chem. Phys.* **2010**, *132*, 154104; b) S. Grimme, S. Ehrlich, L. Goerigk, *J. Comput. Chem.* **2011**, *32*, 1456.

[20] E. R. Johnson, A. D. Becke, *J. Chem. Phys.* **2005**, *123*, 024101.

[21] a) E. van Lenthe, E. J. Baerends, J. G. Snijders, *J. Chem. Phys.* **1993**, *99*, 4597; b) E. van Lenthe, E. J. Baerends, J. G. Snijders, *J. Chem. Phys.* **1994**, *101*, 9783; c) E. van Lenthe, A. Ehlers, E. J. Baerends, *J. Chem. Phys.* **1999**, *110*, 8943.

[22] N. Mardirossian, M. Head-Gordon, *Mol. Phys.* **2017**, *115*, 2315.

[23] E. van Lenthe, E. J. Baerends, *J. Comput. Chem.* **2003**, *24*, 1142.

[24] a) M. Franchini, P. H. T. Philipsen, L. Visscher, *J. Comput. Chem.* **2013**, *34*, 1819; b) M. Franchini, P. H. T. Philipsen, E. van Lenthe, L. Visscher, *J. Chem. Theory Comput.* **2014**, *10*, 1994.

[25] a) A. Klamt, G. Schüürmann, *J. Chem. Soc. Perkin Trans. 2* **1993**,799; b) A. Klamt, *J. Phys. Chem.* **1995**, *99*, 2224; c) A. Klamt, V. Jonas, *J. Chem. Phys.* **1996**, *105*, 9972; d) C. C. Pye, T. Ziegler, *Theor. Chem. Acc.* **1999**, *101*, 396.